


Article

# Experimental Investigation on CO<sub>2</sub> Methanation Process for Solar Energy Storage Compared to CO<sub>2</sub>-Based Methanol Synthesis

Beatrice Castellani <sup>1,\*</sup> , Alberto Maria Gambelli <sup>1</sup>, Elena Morini <sup>1</sup>, Benedetto Nastasi <sup>2</sup>, Andrea Presciutti <sup>1</sup>, Mirko Filipponi <sup>1</sup>, Andrea Nicolini <sup>1</sup> and Federico Rossi <sup>1</sup>

<sup>1</sup> Engineering Department, University of Perugia, CIRIAF, Via G. Duranti 67, 06125 Perugia, Italy; albertomaria.gambelli@studenti.unipg.it (A.M.G.); morini@crbnet.it (E.M.); andrea.presciutti@unipg.it (A.P.); mirko.filipponi@unipg.it (M.F.); andrea.nicolini@unipg.it (A.N.); federico.rossi@unipg.it (F.R.)

<sup>2</sup> Department of Architectural Engineering & Technology, Environmental & Computational Design Section, TU Delft University of Technology, Julianalaan 134, 2628 BL Delft, The Netherlands; benedetto.nastasi@outlook.com

\* Correspondence: beatrice.castellani@unipg.it

Received: 18 May 2017; Accepted: 21 June 2017; Published: 27 June 2017

**Abstract:** The utilization of the captured CO<sub>2</sub> as a carbon source for the production of energy storage media offers a technological solution for overcoming crucial issues in current energy systems. Solar energy production generally does not match with energy demand because of its intermittent and non-programmable nature, entailing the adoption of storage technologies. Hydrogen constitutes a chemical storage for renewable electricity if it is produced by water electrolysis and is also the key reactant for CO<sub>2</sub> methanation (Sabatier reaction). The utilization of CO<sub>2</sub> as a feedstock for producing methane contributes to alleviate global climate changes and sequestration related problems. The produced methane is a carbon neutral gas that fits into existing infrastructure and allows issues related to the aforementioned intermittency and non-programmability of solar energy to be overcome. In this paper, an experimental apparatus, composed of an electrolyzer and a tubular fixed bed reactor, is built and used to produce methane via Sabatier reaction. The objective of the experimental campaign is the evaluation of the process performance and a comparison with other CO<sub>2</sub> valorization paths such as methanol production. The investigated pressure range was 2–20 bar, obtaining a methane volume fraction in outlet gaseous mixture of 64.75% at 8 bar and 97.24% at 20 bar, with conversion efficiencies of, respectively, 84.64% and 99.06%. The methanol and methane processes were compared on the basis of an energy parameter defined as the spent energy/stored energy. It is higher for the methanol process (0.45), with respect to the methane production process (0.41–0.43), which has a higher energy storage capability.

**Keywords:** CO<sub>2</sub> methanation; carbon recycling; energy storage; solar energy; P2G Power to Gas; synthetic fuels

## 1. Introduction

The environmental and economic sustainability of future energy systems needs to deal with several challenges and technical aspects. The increase of the share of Renewable Energy Sources (RES) overcame 25% of energy generation, implying new issues related to balancing, security, and production-consumption profiles matching [1]. While the existing electricity network results were largely unchanged, solar and wind power have seen a large expansion during the last decade. This means that the current electrical energy system is un-optimized and needs adjustments.

The electricity transmission system needs to be adapted from the large scale production facilities used today to smaller and locally distributed energy production sites. Energy storage solutions are

being implemented to compensate for the fluctuations in intermittent energy production [2]. Recent investigations indicate that the introduction of energy storage technologies [3,4] and routes can help to stabilize power output while also enhancing the reliability of renewable energy production [5].

Then, excess electricity from renewable energy sources (RES) has to be stored in different ways such as in batteries or be used to produce hydrogen ( $H_2$ ) [6]. Solar energy is the first renewable source associated with  $H_2$  production as a storage medium, especially for the shift from daytime production to nighttime demand or the seasonal shift from summer overproduction to winter needs [7]. Hydrogen-based energy storage systems have proven to be one of the most promising energy storage techniques [8]. A further proof is the extensive research in stand-alone application, such as in [9].

Research on hydrogen technologies has been facing many challenges, including production, storage, and transportation infrastructure [10,11]. It is noteworthy that hydrogen is already proven in current gas grid pipelines and even, in certain fractions, used in well-established end-user devices such as boilers and cookers [12]. Indeed, new measurement procedures for conventional systems were studied [13]. Thus there are numerous efforts underway to develop better ways of producing  $H_2$ , especially via the enhanced electrolysis of water [14].

Moreover, concerns about climate change as well as fossil fuel usage motivate  $CO_2$  sequestration technologies in order to limit the emissions without substantially changing the well-proven technologies already in use [15]. Nevertheless, the main drawback is to handle the captured and stored  $CO_2$  as a waste to be disposed of [16].

To overcome this vision, recovering and combining two waste materials such as renewable excess electricity and  $CO_2$  is the key driver to further foster RES production and increase its share in the national energy mix as well as to make our energy carbon footprint smaller by means of synthetic fuel production. RES capacity firming can be mitigated and solved by means of feeding electrolyzers to produce  $H_2$  to address a single energy network or to create synergies among electricity, heating [17], and even transport purposes. Thus  $H_2$  can be combined by thermo-chemical processes with the  $CO_2$  coming from existing power plants equipped with Carbon Capture and Storage (CCS) solutions. In this way, the resulting fuels could again feed the energy generation side and, consequently, reduce the energy-related emissions [18]. Thus,  $H_2$ - $CO_2$  combination-derived fuels would, by connecting different energy sectors, make the system more flexible and recycle  $CO_2$  as a carbon source and, by implementing electrolyzers, help balance the Grid and facilitate high RES power integration towards smart energy systems [19].

Moreover,  $CO_2$  can be captured by a biomass gasification process and recombined with the  $H_2$ -rich gas [20] to obtain fuels and olefins in poly-generation systems [21]. Among those products, methanol is receiving attention by researchers as a possible carbon recycling strategy [22], but further analysis is required when the production and the energy generation is evaluated from an economic perspective within the new multi-energy systems layout [23].

The main issue of this is related to the absence of dedicated infrastructures, while, for natural gas these are well established and capillary in many countries. Hence, the interest in synthesizing methane by the combination of  $H_2$ - $CO_2$  is supported by the chance to use it as a raw material for other uses or products [24].

This paper focuses on the above-mentioned strategy; the utilization of  $CO_2$  as a feedstock, together with renewable hydrogen, for synthetic fuel production. An experimental apparatus was assembled and used for an investigation on the  $CO_2$  methanation for synthetic methane production. Methane is already a core supply of energy systems worldwide, with huge amounts of physical and knowledge infrastructure [25]; it is easy to store and boasts an energy density around three times greater than hydrogen. The experimental results were used to compare the methane production process with the methanol production process. For both the routes, the ratio between the energy spent throughout the process to produce the fuel and the energy stored in the fuel is calculated.

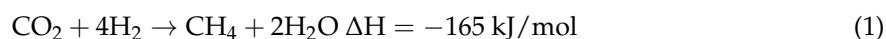
This parameter is introduced to quantify the performances of the above storage systems with the aim of determining the best available technology throughout the whole chain, from hydrogen production to the delivery of fuel for final use.

Foreseeable opportunities are related to the mixing of synthetic fuel coming from different production chains so as to integrate renewable electricity excess, flue gas, and Carbon Capture and Storage solutions together with forthcoming bio-refineries concepts and promising algae treatments [26].

## 2. Process Description

### 2.1. Methane Production

The methane-based process is based on the transformation of electrical energy to synthetic natural gas by means of an electrolyzer and creating the conditions suitable for the Sabatier reaction. The Sabatier reaction combines carbon dioxide and hydrogen to produce methane and water in the reaction (Equation (1)):



This reaction is exothermic and is limited by the thermodynamic equilibrium. The operating temperatures are typically around 250–400 °C. The Sabatier reaction has been widely investigated because of its potential to allow CO<sub>2</sub> to be captured and recycled, to store energy from renewable sources used to feed the electrolyzer for producing H<sub>2</sub>, and, subsequently, for CH<sub>4</sub> to be injected and stored in existing natural gas grids or used as a fuel for transportation.

The process is mainly composed by two stages; (i) an electrolyzer, supplied by the electric energy and (ii) a Sabatier reactor for the conversion of hydrogen into methane (Figure 1).

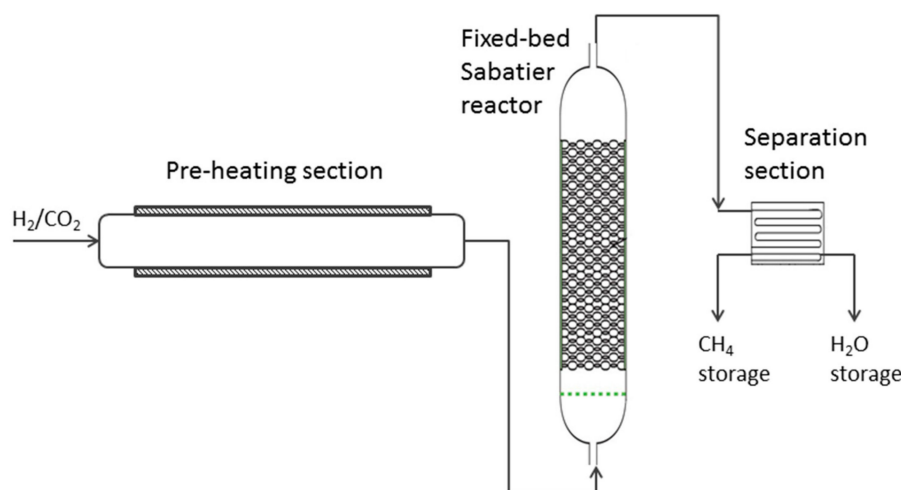


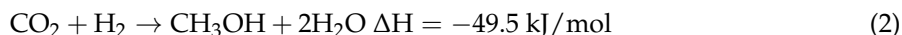
**Figure 1.** Scheme of the CO<sub>2</sub> methanation process.

### 2.2. Methanol Production

Methanol is a primary liquid petrochemical that has attracted considerable attention in the chemical and energy industries. The production of methanol used as a fuel and a chemical has been proposed in the methanol economy by [27].

Two main aspects of this new economy are underlined. CO<sub>2</sub> can be captured and transformed into methanol allowing the costs for CO<sub>2</sub> sequestration to be avoided and CO<sub>2</sub> to be effectively recycled. The process also has great industrial significance because the product, methanol, can serve as a liquid fuel as well as a raw material for the synthesis of other organic compounds [28].

The reaction of the conversion of the CO<sub>2</sub> to CH<sub>3</sub>OH is as in Equation (2):



The methanol-based process is based on the use of hydrogen in the conversion of electrical energy to methanol by the use of CO<sub>2</sub>. Electrical energy and water are included in the process to produce hydrogen that reacts with CO<sub>2</sub> and results in methanol.

The reaction is highly exothermic; therefore it is facilitated at a high pressure and low temperature. CO<sub>2</sub> is converted to methanol in the temperature range of 250–300 °C and pressure range of 5–10 MPa using CuO/ZnO/Al<sub>2</sub>O<sub>3</sub> as a catalyst. The produced methanol CH<sub>3</sub>OH is liquid at ambient temperature and can be safely stored and handled.

The process is mainly composed by two stages: (i) an electrolyzer, supplied by electrical energy and (ii) a reactor for the conversion of CO<sub>2</sub> and hydrogen into methanol (Figure 2).

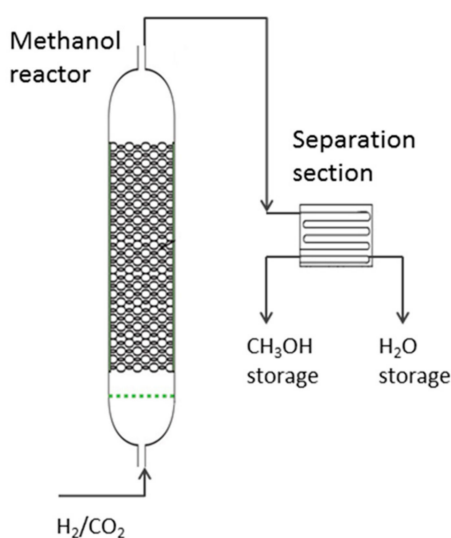


Figure 2. Scheme of methanol-based process.

### 3. Experimental Section

This section describes the experimental setup and gives data about the used materials.

#### 3.1. Experimental Setup

The experimental apparatus includes the following sections; an electrolyzer, a CO<sub>2</sub>-H<sub>2</sub> mixing section, a heating section, a Sabatier reactor, and a water separation section. Hydrogen is produced by an electrolyzer, supplied by Erredue Srl (G Series H0<sub>3</sub>, Erredue Srl, Livorno, Italy), and is then mixed with CO<sub>2</sub> according to the stoichiometric proportion (Equation (1)). The electrolyzer, shown in Figure 3, operates at a pressure of 2.5 bar and produces a maximum hydrogen flowrate of 2.5 Nm<sup>3</sup>/h. H<sub>2</sub>/CO<sub>2</sub> mixing occurs through a T piping. Gas flows are measured and controlled by digital thermal mass flow meters (El-flow Series), supplied by Bronkhorst. Mass flow meters have the following characteristics: flow rate in the range from 0.08 to 4 Nm<sup>3</sup>/h; maximum inlet pressure 30 bar; control stability lower than ±0.1% Full Scale (FS); and temperature sensitivity lower than 0.05% FS/°C. The gaseous mixture flows with a rate of 0.63 m<sup>3</sup>/h through the two chambers (pre-heater and reactor). The heating section is constituted by a horizontal tube with a nominal diameter of 25.4 mm (1 inch) and a length of 300 mm on which three mineral insulated band heaters are mounted. It is equipped with internal temperature and pressure sensors and is connected to the Sabatier reactor through a gate valve (supplied by Swagelok, model SS-6nbs 10 mm-G), suitable for a maximum temperature of 640 °C.



**Figure 3.** Electrolyzer G Series H0<sub>3</sub> supplied by Erredue Srl.

The Sabatier reactor is a cylindrical AISI 304 stainless monotubular fixed bed reactor with a diameter of 1 inch (25.4 mm) and a length of 300 mm. It is filled with Ni catalyst pellets. The reactor is equipped with one pressure sensor and one temperature sensor. The pressure sensor is a Bourdon Tube pressure gauge (NG100 series, Kobold Messring GmbH, Hofheim am Taunus, Germany), supplied by Kobold (accuracy class 1), with a pressure range from 0 to 40 bar. The temperature sensors are mineral insulated type K thermocouples (accuracy class 1).

For reducing heat loss and for safety reasons, the two chambers were coated with thermo-insulating material and an external protective aluminium coating. The band heaters are provided by Watlow and have the following technical characteristics: length of 63.5 mm, internal diameter of 32 mm, power of 700 W, and internal K thermocouple. The band heaters are controlled by Proportional–Integral–Derivative (PID) regulators mounted on a control panel.

The reaction products pass then through the water separation section, constituted by a 6 mm stainless steel cooling coil immersed in a thermostatic bath. In this section, water vapor condensation occurs, and the gaseous incondensable products are collected for gascromatographic analysis. The installation of the experimental apparatus is shown in Figure 4. Voltage signals from the sensors are collected by software for data acquisition on a personal computer every 5 s.



**Figure 4.** Experimental apparatus for CO<sub>2</sub> methanation process.



Gas-chromatographic analyses are carried out with a gas-chromatographer supplied by VARIAN (model VARIAN CP 4900 Micro-GC, VARIAN Inc., Middelburg, The Netherlands). It is configured to use helium (He) and Argon (Ar) as carriers, with a minimum purity of 99.995%. The gas-chromatographer has: (i) four columns, including Molsieve MS5A, working with Argon and Poraplot PPU, CPSil 5CB, Molsieve MS5A, working with Helium; and (ii) a thermal conductivity detector (TCD). This detector responds to differences in thermal conductivity between the carrier gas and each component of the analyzed gas mixture. When a particular component goes through the TCD, the signal shows a deviation, the entity of which is proportional to that component concentration.

The measurements, periodically carried out with certified mixtures, show that the uncertainties are always lower than 1%, with an excellent repeatability on sequences of samples [16].

### 3.2. Materials

The Sabatier reaction is catalyzed by Ni-based catalyst supplied by BASF (G1-85 T5x5, BASF Corporation, Erie, PA, USA). BASF G1-85 Ni/Zr/Al<sub>2</sub>O<sub>3</sub> Catalyst contains metallic nickel and zirconium on an alumina support: the nickel content in weight is 50%. The catalyst is supplied in 1 mm × 4 mm cylindrical pellets, with a specific surface area of 123 m<sup>2</sup>/g. The catalyst is suitable for the methanation of synthesis gas received from coal or biomass gasification to produce Substitute Natural Gas (SNG). Under proper conditions, lifetimes of more than four years can be achieved.

The catalyst must be converted into the active form to turn nickel to the metallic state, removing the oxide layer from the catalyst surface. Activation was achieved by the following activation process, consistent with [29]. Initially, pure nitrogen was fluxed inside the reactor at a pressure of 1.5 bar, with the aim of removing all the air present inside the two cylinders. The internal temperature was brought to a value of 220 °C, with a heating rate of 60 °C/h. Then, pure hydrogen was fluxed at a pressure of 2 bar through the catalyst, and the system was heated to 430 °C with a heating rate equal to 120 °C/h. Nitrogen and hydrogen (99.999% Alphagaz 1) were supplied by Air Liquide Italia Service (Air Liquide Italia S.p.A., Milan, Italy). The catalyst's activated state can be visually checked by a color change from black, typical of nickel oxide, to dark grey, typical of molecular nickel.

## 4. Experimental Results

The experimental campaign consists of 14 tests. The operating parameters such as the CO<sub>2</sub>/H<sub>2</sub> ratio, flow conditions, temperature, and pressure are shown in Table 1. Tests 1 to 10 were carried out using the stoichiometric H<sub>2</sub>/CO<sub>2</sub> ratio of four, while Tests 11 to 14 with a H<sub>2</sub>/CO<sub>2</sub> ratio equal to one. Tests 1 to 6 and Tests 11 to 14 were carried out continuously, with a hourly space velocity, defined as the ratio between the flowrate and the reactor volume, of 414.4 h<sup>-1</sup>. Tests 7 to 10, instead, were carried out in batch conditions; this means that the inlet CO<sub>2</sub>/H<sub>2</sub> mixture was uploaded inside the reactor until the experimental conditions of temperature and pressure were reached. The reactor was then sealed, and parameters were monitored. The experimental tests were carried out with an initial internal temperature in the range from 250 °C and 451 °C and an initial internal pressure from 2 bar to 20 bar. The temperature and pressure values in Table 1 are referred to as the internal initial conditions, measured inside the reactor at the steady state. The reaction time, which is considered to start from the temperature increase, was equal to 30 min for all the tests.

To better understand the temperature trend during the experimental tests, the profile of the internal temperature during Test 1 is shown in Figure 5. The heating phase is represented in the first part of the graph (0–80 min), during which the reactor reaches the initial experimental temperature of 250 °C. At that point, a sharp increase in temperature occurs. The temperature passes from 268 °C to 403 °C in one minute because of the exothermicity of the Sabatier reaction. After 30 min in which temperature is in the range from 350 °C to 450 °C, it starts to decrease until 300 °C.

Table 1. Experimental test.

Test	CO <sub>2</sub> /H <sub>2</sub> Ratio	Batch or In-Continuo (B-C)	Temperature [°C]	Pressure [bar]
1	1/4	C	250	2
2	1/4	C	317	2
3	1/4	C	363	4
4	1/4	C	490	4
5	1/4	C	422	8
6	1/4	C	451	20
7	1/4	B	250	10
8	1/4	B	271	10
9	1/4	B	350	10
10	1/4	B	353	15
11	1/1	C	371	16
12	1/1	C	325	17
13	1/1	C	329	17
14	1/1	C	378	17

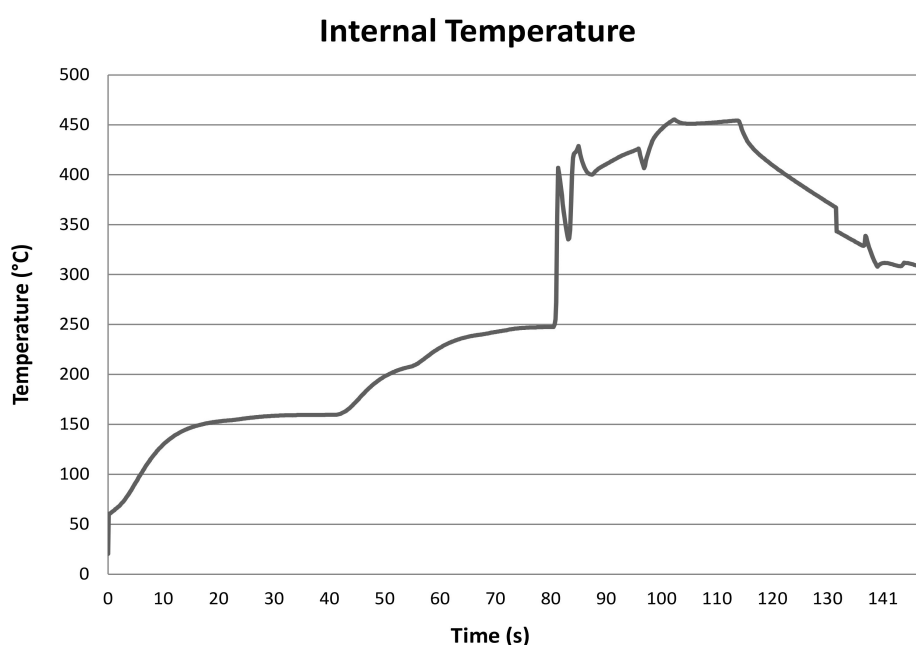


Figure 5. Temperature profile during Test 1.

In all tests, after the heating phase, there is a 1-minute rapid temperature increase when the reaction occurs. After 30 min since the temperature increase, the conversion process is considered completed and the outlet gaseous mixture is collected to be analyzed at the gas-chromatographer. In Table 2, for each test, the composition of the gaseous mixture collected at the end of the process is shown, together with the conversion percentage of the reactants.

Comparing the results of Tests 1 to 6, which were carried out in-continuo with the stoichiometric CO<sub>2</sub>/H<sub>2</sub> ratio, there is an increase in the methane volume fraction when pressure has the same trend. In particular, at 2 bar, the methane volume fraction is equal to 8.55%, while Test 5 at 8 bar shows the best result at low pressures (64.75%). Test 6 at high pressure (20 bar) reaches 97.24% methane content. The highest conversion efficiencies are obtained in Tests 5 and 6, with, respectively 84.64% and 99.06%.

Tests 7 to 10 lead to negligible methane production because of batch conditions, with consequent low conversion efficiencies (from 6.51% to 31.63%). For this group, the best results were obtained in Tests 9 (13.36%) and 10 (12.52%), carried out at respectively 350 °C and 353 °C, with conversion efficiencies of 31.63% and 30.04% respectively.

Table 2. Experimental results.

Test	Pressure [bar]	Temperature [°C]	Final % v/v			Conversion Efficiency [%]
			H <sub>2</sub>	CH	CO <sub>2</sub>	
1	2	250	85.98	8.55	5.47	21.90
2	2	317	15.53	37.80	46.68	64.58
3	4	363	56.33	29.13	14.54	55.22
4	4	490	72.61	19.47	7.92	42.04
5	8	422	24.58	64.75	10.67	84.64
6	20	451	1.74	97.24	1.02	99.06
7	10	250	58.56	5.99	35.44	16.05
8	10	271	60.57	2.27	37.16	6.51
9	10	350	17.93	13.36	68.71	31.63
10	15	353	29.75	12.52	57.73	30.04
11	16	371	90.65	8.79	0.56	22.43
12	17	325	33.11	32.82	34.08	59.44
13	17	329	11.68	36.60	51.72	63.39
14	17	378	3.96	15.79	80.25	36.00

The last four tests (11–14) were carried out with a CO<sub>2</sub>/H<sub>2</sub> ratio equal to one. The methane volume fraction reaches a value of 36.6%, with a temperature of 329 °C. Significant conversion efficiency is obtained at 325–329 °C (59.44% and 63.39% respectively). Tests 11 and 14, instead, result in a lower methane content with a higher temperature value.

The results, shown in Table 2, allow a discussion of the influence of the operating parameters on the methanation process. The in-continuo operation of the apparatus is clearly the fundamental element to obtain noteworthy results. Tests 11–14 demonstrated the strong conversion decrease caused by a deviation from the ideal value of the CO<sub>2</sub>/H<sub>2</sub> ratio. Since the CO<sub>2</sub> methanation reaction occurs with a decrease in the number of moles, pressure is the key parameter to foster the conversion; it accelerates the reaction and is directly proportional to the methane production rate. Figure 6 clearly shows the positive effect of pressure on the process, with an increasing regression line. The regression line was built on the results of Tests 2, 4, 5, and 6, carried out at different temperatures but in the highest investigated range (300–400 °C). Figure 7 represents the CH<sub>4</sub> volume content as a function of temperatures, using the results of Tests 1 to 6, carried out at pressures from 2 bar to 20 bar. The temperature represents an aid only within its optimal range and has a beneficial action only within the range from 400 to 450 °C.

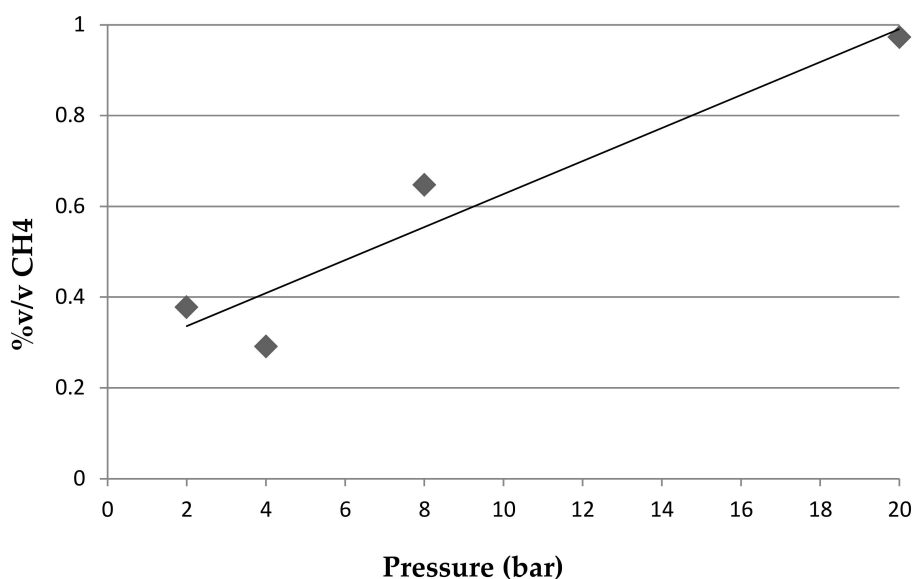


Figure 6. Pressure influence on methane volumetric fraction.



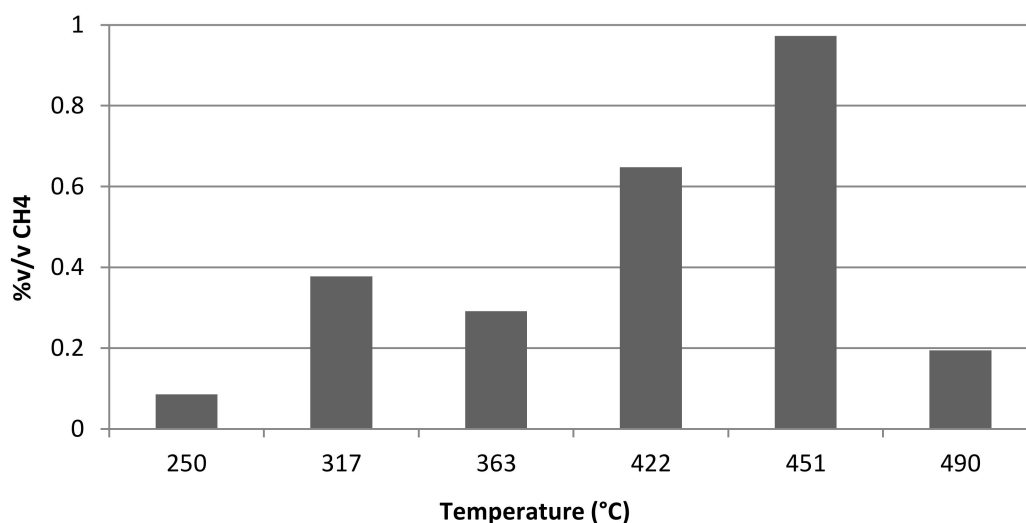


Figure 7. Temperature influence on methane volumetric fraction.

## 5. Energy Evaluation

The experimental methane-based process was compared to the methanol-based process described in Section 2.2 on the basis of an energy parameter defined in Equation (3) [30]:

$$\frac{\text{Spent Energy}}{\text{Stored Energy}} \quad (3)$$

The considered parameter is an adimensional number calculated as the ratio between the specific energy spent in all the sections of the process to produce the fuel in its storing form and the specific energy stored in the fuel, corresponding to the lower heating value.

The total energy involved in the two processes for production of the final fuel in its transportable form was calculated. The total energy involved in the processes consists of:

- hydrogen and carbon dioxide compression for injection in the synthesis reactor,
- energy consumption for heating the reactor to the synthesis temperature,
- removal of reaction heat,
- energy consumption for bringing the fuel to the storing conditions.

The process conditions for both the analyzed cases are summarized in Table 3. The data for electrolysis used in the calculations are those of in-lab G Series H0<sub>3</sub> Electrolyzer.

Table 3. Comparison of experimental results.

Parameter	Methane Process	Methanol Process
Electrolyzer pressure (bar)	2.5	2.5
Synthesis reactor pressure (bar)	20	70
Synthesis reactor temperature (K)	723	673
Reaction heat (kJ/mol)	165	49.5
Conversion efficiency	0.95	0.95
Storage pressure (bar)	200	1
Storage temperature (K)	298	298
Lower heating value (kJ/kg)	50,000	19,700

The energy consumption of the electrolyzer is equal to 3.75 kWh/Nm<sup>3</sup> of hydrogen (13,500 kJ/Nm<sup>3</sup>). For the methane process, the pressure and temperature of the synthesis reactor

were considered as in Test 6 (20 bar and 723 K), while for the methanol process the pressure and temperature data in Table 3 were chosen in accordance with the optimal ranges in the literature, as described in Section 2.2. For both synthesis reactions, stoichiometric CO<sub>2</sub>-H<sub>2</sub> gaseous mixtures were considered. From a volume unit of CO<sub>2</sub>-H<sub>2</sub> mixture in normal conditions and a proportion of 1:4, 0.29 kg of methane is produced. From a volume unit of CO<sub>2</sub>-H<sub>2</sub> mixture in normal conditions and a proportion of 1:3, 0.58 kg of methanol is produced.

To calculate the work of compression, all the compression stages were considered multi-stage adiabatic compressions with inter-cooling, with a compression efficiency of 85%. For all operations of cooling or heating, where the environment can be used as a heat sink or source, the energy consumption was considered equal to zero. For systems that required cooling down to low temperatures, the coefficient of performance (COP) was considered equal to three. This value is consistent with other studies in the literature [30]. In addition, the recovery of heat from compression operations was not considered.

Methane formation and methanol formation are both exothermic reactions. To ensure a constant temperature during the entire process, reaction heat must be removed with a cooling system (COP equal to three). The reaction heat values are reported in Table 3.

Methane produced via Sabatier reaction can be injected into the grid or stored in a compressed form in gas bottles at 200 bar.

In this case, the work of compression for a two-stage adiabatic compression, from 20 bar to 200 bar, is 503 kJ/kg. The energy consumption for intercooling is considered equal to zero since the environment can be a heat sink. The methanol is stored in liquid form at atmospheric pressure and environmental temperature. The energy expenditures calculated in accordance with the above-mentioned considerations are shown in Table 4.

**Table 4.** Energy expenditures.

Energy Consumption (kJ <sub>el</sub> /kg <sub>fuel</sub> )	Methane Process	Methanol Process
Electrolyzer	76,799	30,400
Gaseous mixture compression to Synthesis pressure	2121	1578
Reactor heating	3784	1966
Removal of reaction heat	3438	516
Compression to storing conditions (200 bar)	503	-
Total consumption	86,645	34,460

Electrolysis is the most energy-consuming phase; the energy consumption for hydrogen production is much higher in terms of the fuels' energy content per unit mass and has the same weight for both the processes (88.6% for methane and 88.3% for methanol). Nevertheless, electrolysis has the potential to transform sustainable electrical energy excess into green hydrogen, which can be considered an input raw material for the considered processes. Thus the system boundaries, for the evaluation of the energy storage capability of methane and methanol, include all the phases from the production of the fuel in its final form, excluding the hydrogen production energy consumption. The spent energy is calculated as the sum of gas compression, reactor heating, and reaction heat removal, considering a factor of 0.46, to convert electric energy consumption to primary energy consumption [31]. The spent primary energy is equal to 8827 kJ/kg for methanol, 21,404 kJ/kg for methane compressed at 20 bar, and 20,309 kJ/kg for methane compressed at 20 bar. The primary energy stored as the heating value in the fuel is equal to 19,700 kJ/kg for methanol and 50,000 kJ/kg for methane. The ratio between the spent energy and the stored energy is a relevant parameter of the storage capability of a synthetic fuel since it takes into account the amount of energy spent to store the fuel in its storing conditions with the respect to the energy stored as heating value and recoverable from its combustion: the higher the ratio, the lower the storage capability.

Figure 8 shows the results of the energy calculations. The results show that the ratio between the spent energy and the stored energy is higher for the methanol process (0.45). The methane production process has the best performance in terms of energy storage capability; the ratio of spent energy/stored energy is equal to 0.43 if it is compressed to 200 bar to be stored in gas bottles, while it is 0.41 if it is injected into the grid at 20 bar.

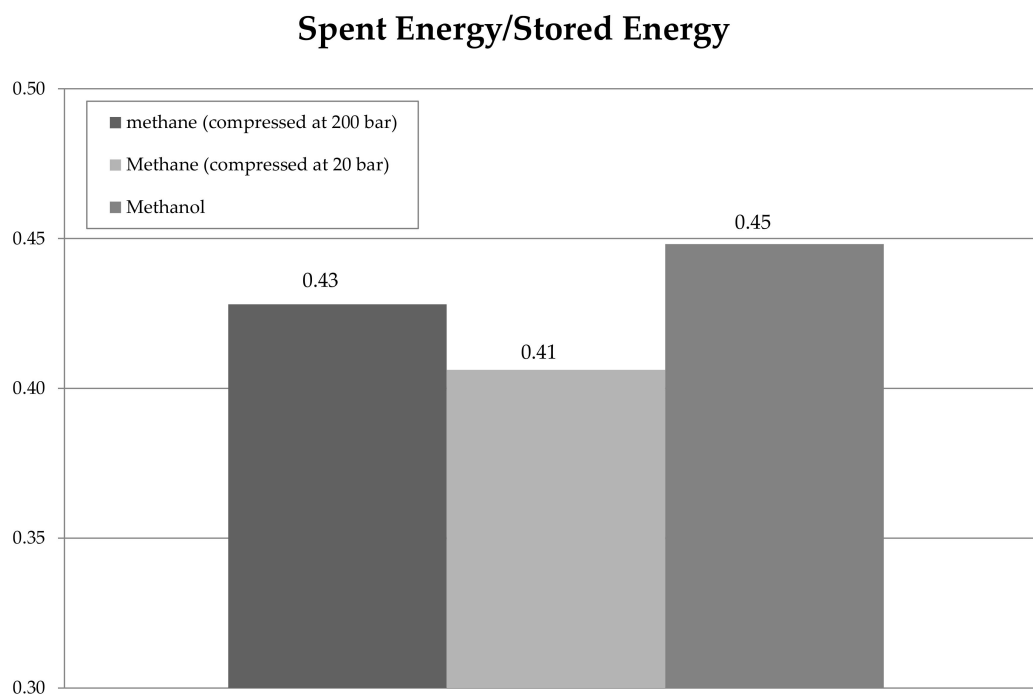


**Figure 8.** Energy performance of the analyzed processes.

## 6. Conclusions

Energy storage systems have gained high interest in research since they are a promising approach to address the challenge of intermittent generation from renewables on the electric grid. For this reason the energy storage industry has continued to evolve and adapt to changing energy requirements and advances in technology. Hydrogen is a very promising energy storage medium since it is a high energy density fuel. Carbon dioxide has been regarded as the biggest contributor to the greenhouse effect, and researchers are working on technologies to allow to industries to capture and reuse waste CO<sub>2</sub> from power generation.

The paper deals with the experimental investigation on the CO<sub>2</sub> methanation process by means of a lab-size apparatus. The investigated pressure range was 2–20 bar, obtaining a methane volume fraction in outlet gaseous mixture of 64.75% at 8 bar and 97.24% at 20 bar, with conversion efficiencies of respectively 84.64% and 99.06%. The influence of the operating parameters on the methanation process was evaluated. A strong conversion decrease occurs with a deviation from the ideal value of the CO<sub>2</sub>/H<sub>2</sub> ratio. Pressure accelerates the reaction and is directly proportional to the methane production rate. The temperature represents an aid within its optimal range.

The performance of the methane-based process was compared with another way of coupling the renewable hydrogen production with the CO<sub>2</sub> recycling; the methanol production process. The two processes were compared on the basis of an energy parameter defined as the spent energy/stored energy. The stoichiometric CO<sub>2</sub>-H<sub>2</sub> gaseous mixtures were considered for both synthesis reactions. The ratio between the spent energy and the stored energy is higher for the methanol process (0.45), with respect to methane production process, which has a spent energy/stored energy ratio equal to

0.41–0.43 depending on the storing compression conditions. Thus the methane production process has the best performance in terms of energy storage capability.

**Acknowledgments:** The authors would like to acknowledge the Italian Ministry of Scientific Research and University for financially supporting the BIT3G project and Novamont for its efforts in coordinating the consortium.

**Author Contributions:** B.C. designed the experiment and conceived and carried out energy analysis. A.M.G. and E.M. performed the experiments. B.N. contributed setting background and data analysis. A.P. contributed instrumentation and data acquisition. B.C. and A.M.G. analyzed the experimental data. M.F. and A.N. contributed analysis tools. B.C., A.M.G., E.M. and B.N. wrote the paper. F.R. supervised the research activities.

**Conflicts of Interest:** The authors declare no conflict of interest. The founding sponsors had no role in the design of the study; in the collection, analyses, or interpretation of data; in the writing of the manuscript; or in the decision to publish the results.

## References

1. Nastasi, B.; Lo Basso, G. Hydrogen to link heat and electricity in the transition towards future Smart Energy Systems. *Energy* **2016**, *110*, 5–22. [[CrossRef](#)]
2. Gallo, A.B.; Simões-Moreira, J.R.; Costa, H.K.M.; Santos, M.M.; Moutinho dos Santos, E. Energy storage in the energy transition context: A technology review. *Renew. Sustain. Energy Rev.* **2016**, *65*, 800–822. [[CrossRef](#)]
3. Castellani, B.; Presciutti, A.; Filipponi, M.; Nicolini, A.; Rossi, F. Experimental investigation on the effect of phase change materials on compressed air expansion in CAES plants. *Sustainability* **2015**, *7*, 9773–9786. [[CrossRef](#)]
4. Rossi, F.; Castellani, B.; Nicolini, A. Benefits and challenges of mechanical spring systems for energy storage applications. *Energy Procedia* **2015**, *82*, 805–810. [[CrossRef](#)]
5. Palizban, O.; Kauhaniemi, K. Energy storage systems in modern grids—Matrix of technologies and applications. *J. Energy Storage* **2016**, *6*, 248–259. [[CrossRef](#)]
6. Sternberg, A.; Bardow, A. Power-to-What?—Environmental assessment of energy storage systems. *Energy Environ. Sci.* **2015**, *8*, 389–400. [[CrossRef](#)]
7. Momirlan, M.; Muresan, L.; Sayigh, A.A.M.; Veziroglu, T.N. The use of solar energy in hydrogen production. *Renew. Energy* **1996**, *9*, 1258–1261. [[CrossRef](#)]
8. Kyriakopoulos, G.L.; Arabatzis, G. Electrical energy storage systems in electricity generation: Energy policies, innovative technologies, and regulatory regimes. *Renew. Sustain. Energy Rev.* **2016**, *56*, 1044–1067. [[CrossRef](#)]
9. Ipsakis, D.; Voutetakis, S.; Seferlis, P.; Stergiopoulos, F.; Elmasides, C. Power management strategies for a stand-alone power system using renewable energy sources and hydrogen storage. *Int. J. Hydrogen Energy* **2009**, *34*, 7081–7095. [[CrossRef](#)]
10. Cotana, F.; Filipponi, M.; Castellani, B. A Cylindrical Molten Carbonate Fuel Cell Supplied with Landfill Biogas. *Appl. Mech. Mater.* **2013**, *392*, 512–516. [[CrossRef](#)]
11. Astiaso Garcia, D.; Barbanera, F.; Cumo, F.; Di Matteo, U.; Nastasi, B. Expert opinion analysis on renewable hydrogen storage systems potential in Europe. *Energies* **2016**, *9*, 963. [[CrossRef](#)]
12. Lo Basso, G.; Nastasi, B.; Astiaso Garcia, D.; Cumo, F. How to handle the Hydrogen enriched Natural Gas blends in combustion efficiency measurement procedure of conventional and condensing boilers. *Energy* **2017**, *123*, 615–636. [[CrossRef](#)]
13. Lo Basso, G.; Paiolo, R. A Preliminary Energy Analysis of a Commercial CHP Fueled with H<sub>2</sub>NG Blends Chemically Supercharged by Renewable Hydrogen and Oxygen. *Energy Procedia* **2016**, *101*, 1272–1279. [[CrossRef](#)]
14. Gentili, P.L.; Penconi, M.; Costantino, F.; Sassi, P.; Ortica, F.; Rossi, F.; Elisei, F. Structural and photophysical characterization of some La<sub>2</sub>xGa<sub>2</sub>yIn<sub>2</sub>zO<sub>3</sub> solid solutions, to be used as photocatalysts for H<sub>2</sub> production from water/ethanol solutions. *Sol. Energ. Mat. Sol. Cells* **2010**, *94*, 2265–2274. [[CrossRef](#)]
15. Castellani, B.; Morini, E.; Filipponi, M.; Nicolini, A.; Palombo, M.; Cotana, F.; Rossi, F. Comparative analysis of monitoring devices for particulate content in exhaust gases. *Sustainability* **2014**, *6*, 4287–4307. [[CrossRef](#)]
16. Castellani, B.; Rossi, F.; Filipponi, M.; Nicolini, A. Hydrate-based removal of carbon dioxide and hydrogen sulphide from biogas mixtures: Experimental investigation and energy evaluations. *Biomass Bioenergy* **2014**, *70*, 330–338. [[CrossRef](#)]

17. De Santoli, L.; Lo Basso, G.; Nastasi, B. The Potential of Hydrogen Enriched Natural Gas deriving from Power-to-Gas option in Building Energy Retrofitting. *Energy Build.* **2017**, *149*, 424–436. [CrossRef]
18. Astiaso Garcia, D. Analysis of non-economic barriers for the deployment of hydrogen technologies and infrastructures in European countries. *Int. J. Hydrogen Energy* **2017**, *42*, 6435–6447. [CrossRef]
19. Nastasi, B. The Eco-Fuels in the Transition Within Energy Planning and Management at Building, District and National Scale Towards Decarbonization Scenarios. Ph.D. Thesis, Sapienza University of Rome, Rome, Italy, 2015.
20. Inayat, A.; Ahmad, M.M.; Yusup, S.; Mutalib, M.I.A. Biomass Steam Gasification with In-Situ CO<sub>2</sub> Capture for Enriched Hydrogen Gas Production: A Reaction Kinetics Modelling Approach. *Energies* **2010**, *3*, 1472–1484. [CrossRef]
21. Salkuyeh, Y.K.; Adams, T.A., II. Co-Production of Olefins, Fuels, and Electricity from Conventional Pipeline Gas and Shale Gas with Near-Zero CO<sub>2</sub> Emissions. Part I: Process Development and Technical Performance. *Energies* **2015**, *8*, 3739–3761. [CrossRef]
22. Elkamel, A.; Reza Zahedi, G.; Marton, C.; Lohi, A. Optimal Fixed Bed Reactor Network Configuration for the Efficient Recycling of CO<sub>2</sub> into Methanol. *Energies* **2009**, *2*, 180–189. [CrossRef]
23. Salkuyeh, Y.K.; Adams, T.A., II. Co-Production of Olefins, Fuels, and Electricity from Conventional Pipeline Gas and Shale Gas with Near-Zero CO<sub>2</sub> Emissions. Part II: Economic Performance. *Energies* **2015**, *8*, 3762–3774. [CrossRef]
24. Caballero, A.; Pérez, P. J. Methane as raw material in synthetic chemistry: The final frontier. *Chem. Soc. Rev.* **2013**, *42*, 8809–8820. [CrossRef] [PubMed]
25. Zhou, X.; Guo, C.; Wang, Y.; Li, W. Optimal Expansion Co-Planning of Reconfigurable Electricity and Natural Gas Distribution Systems Incorporating Energy Hubs. *Energies* **2017**, *10*, 124. [CrossRef]
26. Magdeldin, M.; Kohl, T.; De Blasio, C.; Järvinen, M.; Won Park, S.; Giudici, R. The BioSCWG Project: Understanding the Trade-Offs in the Process and Thermal Design of Hydrogen and Synthetic Natural Gas Production. *Energies* **2016**, *9*, 838. [CrossRef]
27. Olah, G.A.; Goepfert, A.; Surya Prakash, G.K. Chemical recycling of carbon dioxide to methanol and dimethyl ether: From Greenhouse gas to renewable, environmentally carbon neutral fuels and synthetic hydrocarbons. *J. Org. Chem.* **2009**, *74*, 487–498. [CrossRef] [PubMed]
28. Yixiong, Y.; Evans, J.; Rodriguez, J.A.; White, M.G.; Liu, P. Fundamental studies of methanol synthesis from CO<sub>2</sub> hydrogenation on Cu(111), Cu clusters, and Cu/ZnO. *Phys. Chem. Chem. Phys.* **2010**, *12*, 9909–9917. [CrossRef]
29. Barbarossa, V.; Vanga, V. Conversione di CO<sub>2</sub> in Metano. Report Ricerca di Sistema Elettrico. Accordo di Programma Ministero dello Sviluppo Economico—ENEA. 2013. Available online: [http://www.enea.it/it/Ricerca\\_sviluppo/documenti/ricerca-di-sistema-elettrico/combustibili-fossili-ccs/2012/rds-2013-192.pdf](http://www.enea.it/it/Ricerca_sviluppo/documenti/ricerca-di-sistema-elettrico/combustibili-fossili-ccs/2012/rds-2013-192.pdf) (accessed on 21 June 2017).
30. Di Profio, P.; Arca, S.; Rossi, F.; Filipponi, M. Comparison of hydrogen hydrates with existing hydrogen storage technologies: Energetic and economic evaluations. *Int. J. Hydrogen Energy* **2009**, *34*, 9173–9180. [CrossRef]
31. Fritsche, U.R.; Greß, H.-W. *Development of the Primary Energy Factor of Electricity Generation in the EU-28 from 2010–2013*; International Institute for Sustainability Analysis and Strategy: Darmstadt, Germany, 2015.

